EUROGRAPHICS 2026
A. Bönsch and N. Umetani
(Guest Editors)

COMPUTER GRAPHICS *forum*
*Volume 45 (2026), Number 2*
*STAR – State of The Art Report*

# Survey on differential estimators for 3d point clouds Supplementary material

Léo Arnal–Anger[1], Thibault Lejemble[2], David Coeurjolly[3], Loïc Barthe[1] and Nicolas Mellado[1]

[1] IRIT, Université de Toulouse, CNRS, Toulouse INP, UT, Toulouse, France
[2] Cerema, Toulouse, France
[3] CNRS, Université Claude Bernard Lyon 1, INSA Lyon, LIRIS, France

## 1. Additional details for Monge Patch methods

### 1.1. Curvature estimators

Let us remind the expression of W:

$$\begin{aligned} \mathrm{W} &= \mathrm{F_I}^{-1}\mathrm{F_{II}} \\ &= \frac{1}{det(\mathrm{F_I})}\begin{pmatrix} GL-FM & GM-FN \\ -FL+EM & -FM+EN \end{pmatrix}, \end{aligned} \tag{1}$$

with, as expressed in Equation (6) (main document)

$$\mathrm{F_I} = \begin{pmatrix} E & F \\ F & G \end{pmatrix} \qquad \mathrm{F_{II}} = \begin{pmatrix} L & M \\ M & N \end{pmatrix} \tag{2}$$

The expression of the matrix W could be decomposed :

$$GL-FM = \frac{h_{uu}+h_v^2 h_{uu}-h_{uv}h_u h_v}{\sqrt{h_u^2+h_v^2+1}}, \tag{3}$$

$$GM-FN = \frac{h_{uv}+h_v^2 h_{uv}-h_{vv}h_u h_v}{\sqrt{h_u^2+h_v^2+1}}, \tag{4}$$

$$-FL+EM = \frac{h_{uv}+h_u^2 h_{uv}-h_{uu}h_u h_v}{\sqrt{h_u^2+h_v^2+1}}, \tag{5}$$

$$-FM+EN = \frac{h_{vv}+h_u^2 h_{vv}-h_{uv}h_u h_v}{\sqrt{h_u^2+h_v^2+1}}. \tag{6}$$

The partial derivatives of the equation (37) (main document) at $(u,v)=(0,0)$, are:

$$\begin{aligned} h_u &= [\mathbf{u}_\ell]_0\,, \\ h_v &= [\mathbf{u}_\ell]_1\,, \\ h_{uu} &= 2u_{q_a}\,, \\ h_{uv} &= 2u_{q_c}\,, \\ h_{vv} &= 2u_{q_b}\,. \end{aligned} \tag{7}$$

2-Monge

The partial derivatives of the Equation (40) (main document), at $(u,v)=(0,0)$ become

$$\begin{aligned} h_u &= [\mathbf{u}_\ell]_0\,, \\ h_v &= [\mathbf{u}_\ell]_1\,, \\ h_{uu} &= 2a\left[\mathbf{u}_1^{\mathcal{H}}\right]_0^2\,, \\ h_{uv} &= 2a\left[\mathbf{u}_1^{\mathcal{H}}\right]_0\left[\mathbf{u}_1^{\mathcal{H}}\right]_1\,, \\ h_{vv} &= 2a\left[\mathbf{u}_1^{\mathcal{H}}\right]_1^2\,. \end{aligned} \tag{8}$$

PC-MLS

### 1.2. Relation between the Weingarten map and the Hessian matrix

It exists a relation between the Hessian matrix $\mathcal{H}$ and the Weingarten map W. The decomposition of W under the assumption $\mathrm{P}(\mathbf{x})=\mathrm{T}(\mathbf{x})$ leads to the decomposition of the Hessian matrix $\mathcal{H}$. Given $h_u = h_v = 0$ in that case, W is decomposed as :

$$GL-FM = h_{uu}, \tag{9}$$

$$GM-FN = h_{uv}, \tag{10}$$

$$-FL+EM = h_{uv}, \tag{11}$$

$$-FM+EN = h_{vv}. \tag{12}$$

With $det(\mathrm{F_I})=1$ due to $E=1$, $F=0$ and $G=1$,

$$\begin{aligned} \mathrm{W} &= \begin{bmatrix} h_{uu} & h_{uv} \\ h_{uv} & h_{vv} \end{bmatrix}, \\ &= \mathcal{H}. \end{aligned} \tag{13}$$

## 2. Fundamental forms computation of `3DQuadric`

Let us remind the formulation of the 3D implicit quadric surface, for $\mathbf{x}=[x,y,z]^T$:

$$\begin{aligned} f(x,y,z) &= ax^2+by^2+cz^2 \\ &\quad +exy+fyz+gxz \\ &\quad +lx+my+nz+d \\ &= 0, \end{aligned} \tag{14}$$

with partial derivatives

$$\begin{aligned} f_x &= 2ax + ey + gz + l, \\ f_y &= 2by + ex + fz + m, \\ f_z &= 2cz + fy + gx + n, \\ f_{xx} &= f_{yy} = f_{zz} = 2a, \\ f_{xy} &= f_{yx} = e, \\ f_{yz} &= f_{zy} = f, \\ f_{xz} &= f_{zx} = g. \end{aligned} \tag{15}$$

The coefficients of the first fundamental form are given as:

$$E = 1 + \frac{f_x^2}{f_z^2}, \tag{16}$$

$$F = 1 + \frac{f_x f_y}{f_z^2}, \tag{17}$$

$$G = 1 + \frac{f_y^2}{f_z^2}, \tag{18}$$

and the coefficients of the second fundamental form:

$$L = \frac{1}{f_z^2 |\nabla f|} \begin{vmatrix} f_{xx} & f_{xz} & f_x \\ f_{zx} & f_{zz} & f_z \\ f_x & f_z & 0 \end{vmatrix}, \tag{19}$$

$$M = \frac{1}{f_z^2 |\nabla f|} \begin{vmatrix} f_{xy} & f_{yz} & f_y \\ f_{zx} & f_{zz} & f_z \\ f_x & f_z & 0 \end{vmatrix}, \tag{20}$$

$$N = \frac{1}{f_z^2 |\nabla f|} \begin{vmatrix} f_{yy} & f_{yz} & f_y \\ f_{zy} & f_{zz} & f_z \\ f_y & f_z & 0 \end{vmatrix}, \tag{21}$$

with $|\nabla f| = \sqrt{f_x^2 + f_y^2 + f_z^2}$.

## 3. Normal estimation on *PCPNet dataset*

As detailed in Section IV-D (main document), most data-driven approaches require a constant number of points as input. In Table 1, we report the error of normal estimators on the *PCPNet dataset* using $k$NN queries, and compare with reference values from [LZM*23]. On this dataset, learning-based approaches provide good results when data is not perturbed by any noise. When adding noise, all approaches give more comparable results. Computation times are not reported for learning-based approaches, however they remain by construction more computationally expensive than the estimators reviewed in this survey, and require a training stage.

## References


[BM16] BOULCH A., MARLET R.: Deep learning for robust normal estimation in unstructured point clouds. In *Eurographics Symposium on Geometry Processing* (2016), vol. 35. doi:10.1111/cgf.12983. 3

[BSG20] BEN-SHABAT Y., GOULD S.: Deepfit: 3d surface fitting via neural network weighted least squares, 2020. doi:10.1007/978-3-030-58452-8_2. 3

[CGBG13] CHEN J., GUENNEBAUD G., BARLA P., GRANIER X.: Non-oriented mls gradient fields. *Computer Graphics Forum 32* (2013). doi:10.1111/cgf.12164. 3

[Clo] CloudCompare: 3d point cloud and mesh processing software open source project. https://www.cloudcompare.org/. 5, 6

[CP05] CAZALS F., POUGET M.: Estimating differential quantities using polynomial fitting of osculating jets. *Computer Aided Geometric Design 22* (2 2005), 121–146. doi:10.1016/J.CAGD.2004.09.004. 3

[DB02] DOUROS I., BUXTON B.: Three-dimensional surface curvature estimation using quadric surface patches. *Scanning 2002 Proceedings 44* (2002). 3

[GG07] GUENNEBAUD G., GROSS M.: Algebraic point set surfaces. *ACM Transactions on Graphics 26* (7 2007). doi:10.1145/1276377.1276406. 3

[GKOM18] GUERRERO P., KLEIMAN Y., OVSJANIKOV M., MITRA N. J.: Pcpnet learning local shape properties from raw point clouds. *Computer Graphics Forum 37* (2018), 75–85. doi:10.1111/CGF.13343. 3

[Gra98] GRAY A.: Modern differential geometry of curves and surfaces with mathematica (second edition). *Computers & Mathematics with Applications 36* (1998). doi:10.1016/s0898-1221(98)91133-6. 3

[HJ87] HOFFMAN R., JAIN A. K.: Segmentation and classification of range images. *IEEE Transactions on Pattern Analysis and Machine Intelligence PAMI-9*, 5 (1987), 608–620. doi:10.1109/TPAMI.1987.4767955. 3

[HJP*24] HANSEN L. H., JENSEN S. B., PHILIPSEN M. P., MØGELMOSE A., BODUM L., MOESLUND T. B.: OpenTrench3D: A photogrammetric 3d point cloud dataset for semantic segmentation of underground utilities. In *2024 IEEE/CVF Conference on Computer Vision and Pattern Recognition Workshops (CVPRW)* (2024), pp. 7646–7655. doi:10.1109/CVPRW63382.2024.00760. 6

[HSL*17] HACKEL T., SAVINOV N., LADICKY L., WEGNER J. D., SCHINDLER K., POLLEFEYS M.: SEMANTIC3D.NET: A NEW LARGE-SCALE POINT CLOUD CLASSIFICATION BENCHMARK. *ISPRS Annals of the Photogrammetry, Remote Sensing and Spatial Information Sciences IV-1/W1* (2017), 91–98. doi:10.5194/isprs-annals-IV-1-W1-91-2017. 5

[LCBM21] LEJEMBLE T., COEURJOLLY D., BARTHE L., MELLADO N.: Stable and efficient differential estimators on oriented point clouds. *Computer Graphics Forum 40* (8 2021), 205–216. doi:10.1111/CGF.14368. 3

[LFS*23] LI Q., FENG H., SHI K., GAO Y., FANG Y., LIU Y.-S., HAN Z.: SHS-Net: Learning signed hyper surfaces for oriented normal estimation of point clouds. In *Proceedings of the IEEE/CVF Conference on Computer Vision and Pattern Recognition (CVPR)* (Los Alamitos, CA, USA, June 2023), IEEE Computer Society, pp. 13591–13600. doi:10.1109/CVPR52729.2023.01306. 3

[LSY24] LYU B., SHEN L.-Y., YUAN C.-M.: Igf-fit: Implicit gradient field fitting for point cloud normal estimation. *Graphical Models 133* (2024), 101214. doi:10.1016/j.gmod.2024.101214. 3

[LZM*23] LI S., ZHOU J., MA B., LIU Y.-S., HAN Z.: Neaf: learning neural angle fields for point normal estimation. In *Proceedings of the AAAI Conference on Artificial Intelligence* (2023), AAAI Press. doi:10.1609/aaai.v37i1.25224. 2, 3

[Pra87] PRATT V.: Direct least-squares fitting of algebraic surface. *Computer Graphics (ACM) 21* (1987). doi:10.1145/37402.37420. 3

[PWY*07] POTTMANN H., WALLNER J., YANG Y. L., LAI Y. K., HU S. M.: Principal curvatures from the integral invariant viewpoint. *Computer Aided Geometric Design 24* (11 2007), 428–442. doi:10.1016/J.CAGD.2007.07.004. 3

[RB25] RAUCH L., BRAML T.: Rohbau3D: A shell construction site 3d point cloud dataset. *Scientific Data 2025 12:1 12* (8 2025), 1478–. doi:10.1038/s41597-025-05827-7. 4

[RGRG15] RIDEL B., GUENNEBAUD G., REUTER P., GRANIER X.: Parabolic-cylindrical moving least squares surfaces. *Computers and Graphics (Pergamon) 51* (2015). doi:10.1016/j.cag.2015.05.006. 3

| Methods | *PCPNet dataset* | | | | | |
|---|---|---|---|---|---|---|
| | no noise | low noise | med noise | high noise | gradient | striped |
| | 8.8728 | 9.1203 | **12.2451** | **15.7539** | 9.6004 | 10.1237 |
| `Mean` [PWY*07] | 12.3597 | 12.4663 | 16.5705 | 16.9537 | 15.9523 | 12.139 |
| | 18.0087 | 18.1304 | 19.8126 | 23.6501 | 18.7846 | 20.2551 |
| | 9.4674 | 11.0477 | 23.9191 | 40.6505 | 10.6934 | 10.578 |
| `PCA` [HJ87] | 11.1004 | 12.1115 | 18.7109 | 29.7062 | 11.7058 | 12.5435 |
| | 15.988 | 16.1132 | 18.4838 | 23.4033 | 15.7814 | 18.9893 |
| | 9.9582 | 11.4649 | 23.5972 | 39.9799 | 11.2904 | 11.6535 |
| `2-Monge` [Gra98] | 11.3045 | 12.302 | 18.7449 | 29.281 | 12.0057 | 13.5163 |
| | 15.6588 | 15.832 | 18.5434 | 23.4784 | 15.7862 | 20.5367 |
| | 9.8282 | 11.3334 | 23.6195 | 40.1641 | 11.099 | 11.3839 |
| `PC-MLS` [RGRG15] | 11.234 | 12.2244 | 18.7077 | 29.4202 | 11.884 | 13.2605 |
| | 15.682 | 15.8461 | 18.5112 | 23.437 | 15.7786 | 21.0488 |
| | 10.5535 | 12.7492 | 24.7637 | 36.1456 | 10.3546 | 10.4989 |
| `JetFitting` [CP05] | 12.1548 | 12.737 | 19.667 | 28.3098 | 12.1529 | 12.5774 |
| | 17.6982 | 17.7237 | 19.6298 | 23.4036 | 17.7298 | 20.9279 |
| | 15.59 | 10.843 | 38.9128 | 53.6072 | 18.9855 | 17.7882 |
| `Sphere` [Pra87] | 16.3087 | 12.2239 | 27.6702 | 48.393 | 18.7652 | 18.5795 |
| | 21.753 | 17.6859 | 20.2596 | 28.5186 | 20.3206 | 22.0796 |
| | 9.7072 | 9.2531 | 15.3379 | 20.4642 | 10.9383 | 10.1171 |
| `APSS` [GG07] | 13.5892 | 12.5738 | 16.6118 | 21.2306 | 11.9678 | 11.9652 |
| | 18.9028 | 17.9864 | 19.5163 | 22.685 | 18.2248 | 19.2875 |
| | 8.5039 | 8.5176 | 14.1713 | 18.6605 | 10.5176 | 9.5625 |
| `UnorientedSphere` [CGBG13] | 12.1375 | 10.8804 | 15.0419 | 19.8295 | 11.0302 | 10.8333 |
| | 16.5122 | 15.7339 | 17.3579 | 20.6389 | 15.9593 | 17.415 |
| | 7.8642 | 8.9442 | 17.9726 | 29.0358 | 11.1611 | 8.9731 |
| `ASO` [LCBM21] | 9.4176 | 10.1144 | 16.044 | 23.4611 | 11.3294 | 10.7392 |
| | 15.3155 | 14.719 | 17.2472 | 21.1078 | 15.2138 | 16.6725 |
| | 15.1789 | 15.2875 | 33.1095 | 48.0904 | 18.4306 | 17.8316 |
| `3DQuadric` [DB02] | 14.4754 | 16.0818 | 24.8587 | 40.0321 | 17.1591 | 18.089 |
| | 16.9712 | 19.6917 | 22.7695 | 27.7624 | 18.9992 | 20.3751 |
| `HoughCNN` [BM16] | 10.23 | 11.62 | 22.66 | 33.39 | 11.02 | 12.47 |
| `PCPNet` [GKOM18] | 9.66 | 11.46 | 18.26 | 22.8 | 13.42 | 11.74 |
| `DeepFit` [BSG20] | 6.51 | 9.21 | 16.72 | 23.12 | 7.92 | 7.31 |
| `AdaFit` [ZLD*21] | 5.19 | 9.05 | 16.44 | 21.94 | 5.9 | 6.04 |
| `NeAF` [LZM*23] | 4.2 | 9.25 | 16.35 | 21.74 | 4.88 | 4.89 |
| `SHS-Net` [LFS*23] | **3.49** | **8.43** | 15.73 | 21.05 | **4.17** | **4.45** |
| `IGF-Fit` [LSY24] | 4.42 | 9.58 | 16.43 | 23.88 | 5.04 | 5.29 |
| `Zhou et al.` [ZLW*24] | 4.25 | 8.78 | 16.11 | 21.75 | 4.94 | 5.2 |
| `PointNorm-Net` [ZNZ*25] | 8.69 | 11.32 | 17.58 | 23.93 | 9.62 | 10.33 |

**Table 1:** *RMS angle error on unoriented normal estimations for different radii* $[75, 150, 700]$ *and artifacts. For comparison, the last 9 rows are the results given by their respective paper. Low, med and high noise correspond to a gaussian noise of standard deviation of, respectively,* 0.12%*,* 0.6% *and* 1.2% *of the bounding box diagonal. Gradient and striped correspond to two density variations.*

[ZLD*21] ZHU R., LIU Y., DONG Z., WANG Y., JIANG T., WANG W., YANG B.: AdaFit: Rethinking learning-based normal estimation on point clouds. In *2021 IEEE/CVF International Conference on Computer Vision (ICCV)* (2021), pp. 6098–6107. doi:10.1109/ICCV48922.2021.00606. 3

[ZLW*24] ZHOU J., LI Y., WANG M., LI N., LI Z., WANG W.: Robust point cloud normal estimation via multi-level critical point aggregation. *Visual Computer 40* (10 2024), 7369–7384. doi:10.1007/S00371-024-03532-X/FIGURES/7. 3

[ZNZ*25] ZHANG J., NIE M., ZOU C., LIU J., LIU L., CAO J.: PointNorm-Net: Self-Supervised Normal Prediction of 3D Point Clouds via Multi-Modal Distribution Estimation . *IEEE Transactions on Pat-*

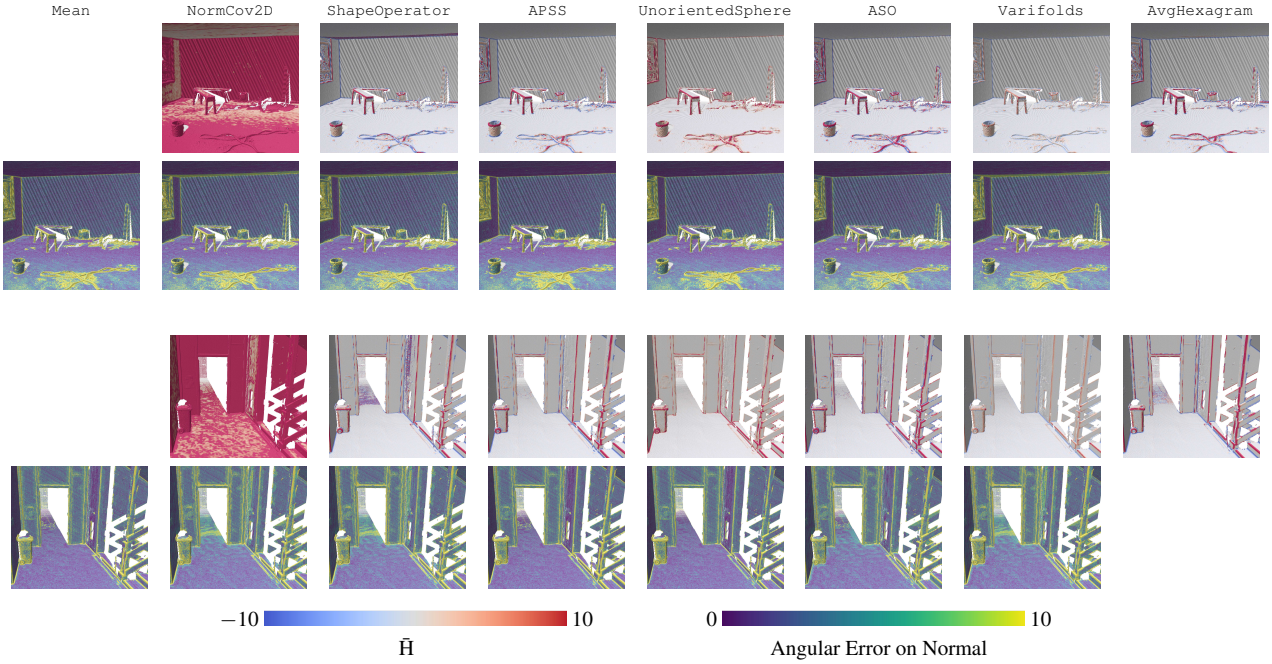


**Figure 1:** *Mean curvature estimation* $\bar{\mathrm{H}}$ *and Angular Error (in degrees) on normals on two 3D indoor scanned models from the* `Rohbaud3D` *dataset [RB25] using a radius of* $r = 0.05m$.

*tern Analysis & Machine Intelligence 47*, 08 (Aug. 2025), 6515–6530.
doi:10.1109/TPAMI.2025.3562051. 3

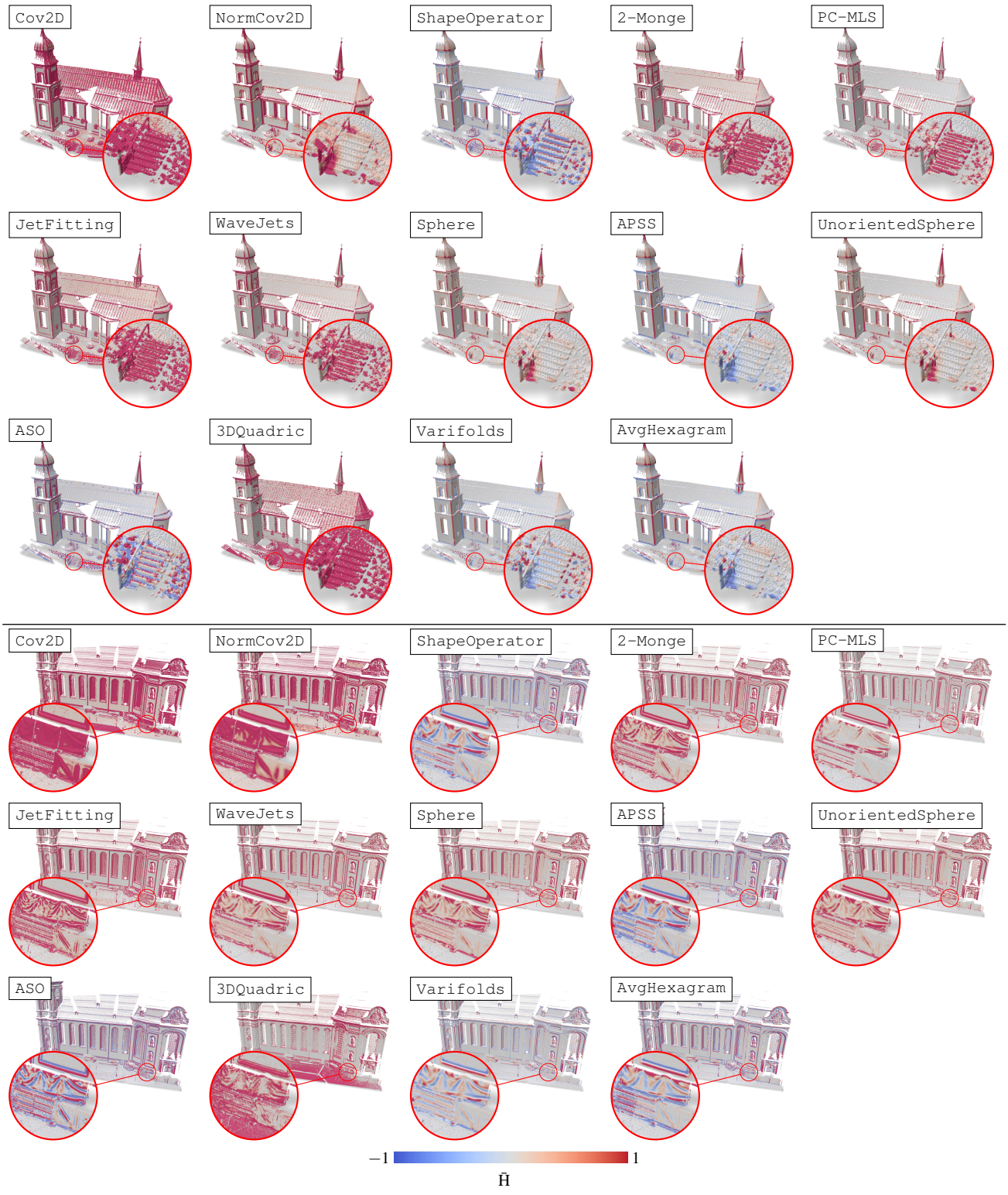


**Figure 2:** *Mean curvature* $\bar{\mathrm{H}}$ *estimation on two cropped 3D scanned models from the* `Semantic3D` *dataset [HSL*17] using a radius of* $r = 0.25m$. *The normals are estimated using* `PCA` *with CloudCompare [Clo].*

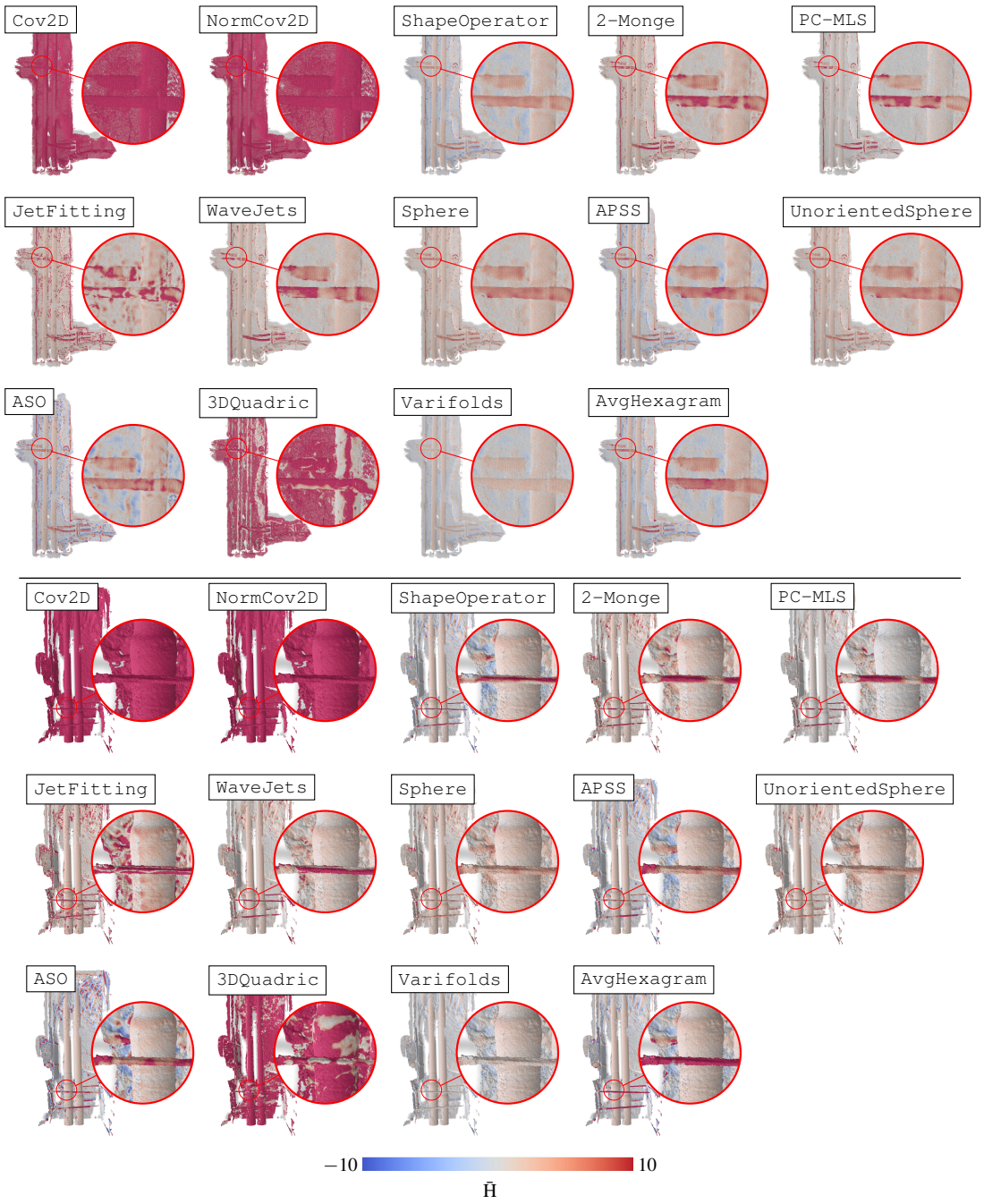


**Figure 3:** *Mean curvature* $\bar{\mathrm{H}}$ *estimation on two 3D scanned models from the* `OpenTrench3D` *dataset [HJP*24] using a radius of* $r = 0.1m$. *The normals are estimated using* `PCA` *on CloudCompare [Clo].*